15th Triennial World Congress, Barcelona, Spain

MODELING THE VST TELESCOPE AND THE EFFECT OF THE WIND DISTURBANCE ON ITS PERFORMANCE

Pietro Schipani, Dario Mancini

Osservatorio Astronomico di Capodimonte
Via Moiariello, 16 - 80131 Napoli - Italy
schipani@na.astro.it

Abstract: The VST (VLT Survey Telescope) is a 2.6 m class Alt-Az telescope to be installed at Mount Paranal in Chile, in the European Southern Observatory (ESO) site. The VST is a wide-field imaging facility planned to supply databases for the ESO Very Large Telescope (VLT) science and carry out stand-alone observations in the UV to I spectral range. So far no telescope has been dedicated entirely to surveys; the VST will be the first survey telescope to start the operation, as a powerful survey facility for the VLT observatory. This paper will focus on the axes motion control system. The dynamic model of the telescope will be analyzed, as well as the effect of the wind disturbance on the telescope performance. The main problems and requirements for a telescope position control will also be discussed. *Copyright © 2002 IFAC*

Keywords: Telescopes, Wind, Tracking, Model

1. ALT-AZIMUTHAL TELESCOPES STAR TRACKING: GENERAL CONCEPTS AND PROBLEMS

The modern optical telescopes are always installed in very good sites for astronomy characterized by excellent weather statistics, no light pollution and a low atmospheric turbulence, usually named “seeing”. Actually due to the atmospheric turbulence the image of a star taken from a ground-based telescope is not a single point but can be seen as a 2-dimension gaussian. A measure of the seeing is the Full Width at Half Maximum (FWHM) of the incident wavefront. The world best astronomical sites (Hawaii, Paranal in Chile, Canary Islands, etc.) have a median seeing of about 0.4-0.7 arcsec (FWHM). These values represent a challenge for the telescope axes control, which are forced to respect very tight tracking requirements in order to have an image quality affected only by the seeing, and so to fully exploit the high quality of such sites. The complexity of the tracking problem is increased by the Alt-Az mounting of all new generation telescopes (e.g. the VST, Fig. 1), compared to traditional "equatorial" telescopes. The Alt-Az telescope mount causes the movement of the main axes around two orthogonal axes: the vertically oriented Azimuth axis, intersecting both zenith and nadir points, and the horizontally oriented Altitude axis. The coordinates of the telescope are different from the ones the astronomers are traditionally used, i.e. Right Ascension and Declination. By the axes control point of view, the tracking of a star is easier in a traditional equatorial mount. In the equatorial mount case the declination axis is not moving after the pointing phase (in which the telescope moves to a new object) and only the right ascension axis must be moved at low and constant speed (15 arcsec/sec) in order to compensate for the earth rotation. On the contrary an Alt-Az mount telescope must follow speed and acceleration variant trajectories. As in any axis control, tracking a trajectory p(t) within tight precision requirements becomes more difficult when high speeds and/or accelerations are required to the system; on the contrary it is easier to follow stationary trajectories. The very slow apparent motion of a star in the sky generally leads to believe that the telescope axes should move very slowly too. This is not always the case in an Alt-Azimuthal mount. In the zenith approaching phase both azimuth speed and acceleration increase up to very high values (∞ at the zenith); therefore a so called “blind spot”, i.e. a little area near the zenith point, must be set, in which the telescope cannot track the star due to the physical constraints of the axes actuators. Anyway in most of the observation nights with an Alt-Az telescope no axis have to track trajectories requiring significant accelerations, but azimuth must often assume significant speeds during observations, whenever the star is “high” in the sky.

2. VST TELESCOPE DYNAMIC MODEL

The telescope coupling dynamic is so slow that it is possible to study independently the two axis

behaviors. The coupling of the two axes is usually negligible in a telescope, especially in the most important operating condition, i.e. the tracking phase, in which the axes trajectory is most of the time regular and not interested by strong accelerations. Both axes structures are modeled by a number of inertias joined by stiffnesses and structural dampings (Fig. 2 shows the altitude axis simplified model, the meaning of the symbols is reported in table 1). The axis gear is represented by the motor and teeth contact stiffness and by the damping. Four motors per axis are used in a symmetrical configuration, implementing a preload scheme which makes negligible the gear backlash. The inertia of the motor itself is taken into account, properly scaled by the transmission ratio. The structural data are derived from a FEA of the mechanical structure of the telescope.

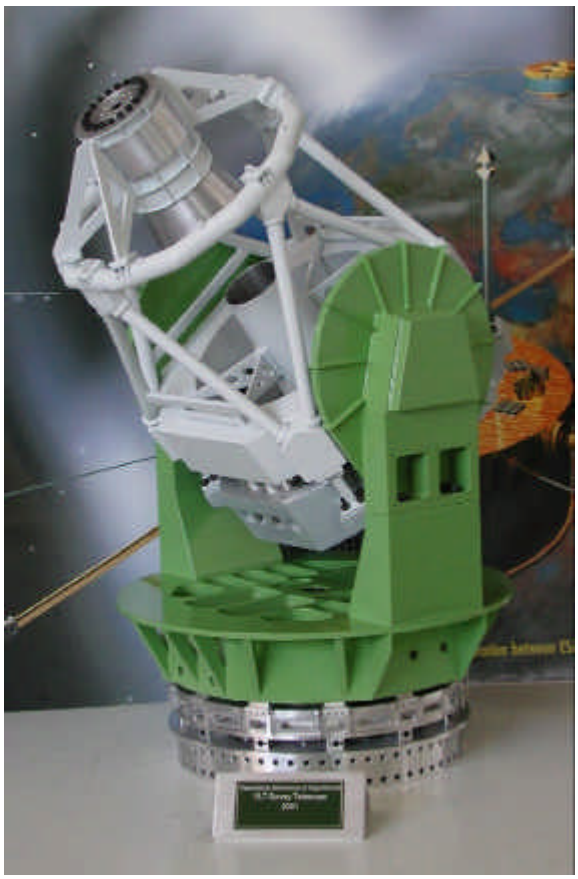

Fig. 1 – VST 1:13 model

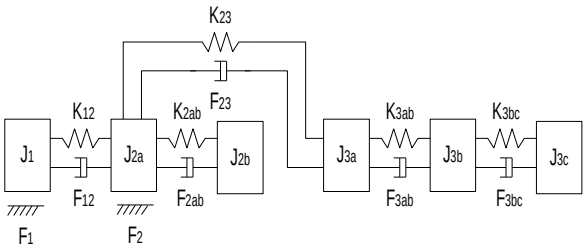

Fig. 2 - Altitude axis model

Table 1 - Altitude axis structural parameters

Parameter	**Symbol**
Center Piece inertia [kg·m^2]	J2a
M1 (Primary Mirror) inertia [kg·m^2]	J2b
Top Ring Inertia [kg·m^2]	J3a
M2 (Secondary Mirror) box Inertia [kg·m^2]	J3b
M2 Inertia [kg·m^2]	J3c
Motors inertia [kg·m^2]	J1
Motors viscous friction [Nm/(rad/s)]	F1
Viscous friction [Nm/(rad/s)]	F2
Transmission damping [Nm/(rad/s)]	F12
M1 pad damping [Nm/(rad/s)]	F2ab
Structural damping [Nm/(rad/s)]	F23
Top Ring - M2 box damping [Nm/(rad/s)]	F3ab
M2 box - Mirror damping [Nm/(rad/s)]	F3bc
Transmission stiffness [Nm/rad]	K12
M1 pad stiffness [Nm/rad]	K2ab
Structural stiffness [Nm/rad]	K23
Top Ring - M2 box stiffness [Nm/rad]	K3ab
M2 box - Mirror stiffness [Nm/rad]	K3bc
Transmission ratio	R

The dynamic of the mechanical system can be described by second order differential equations in matrix form as:

$$J\ddot{\Theta} + F\dot{\Theta} + K\Theta = T \qquad (1)$$

where J, F, K, T are the inertia, viscous damping, stiffness and torque matrix respectively, and Θ is the angular position vector. Fig. 3 shows the open loop response of the altitude axis electromechanical model. Fig. 4 shows the open loop transfer function of the azimuth axis. The first notch in the bode gain plots represents the Locked Rotor eigenfrequency (~10 Hz for both axes).

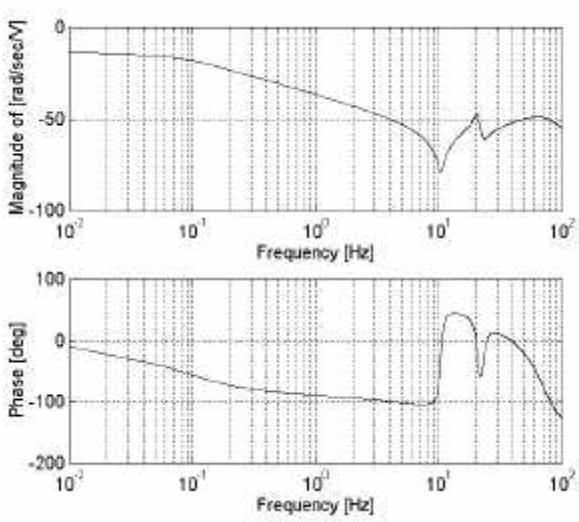

Fig. 3 - Altitude axis: open loop transfer function bode diagram

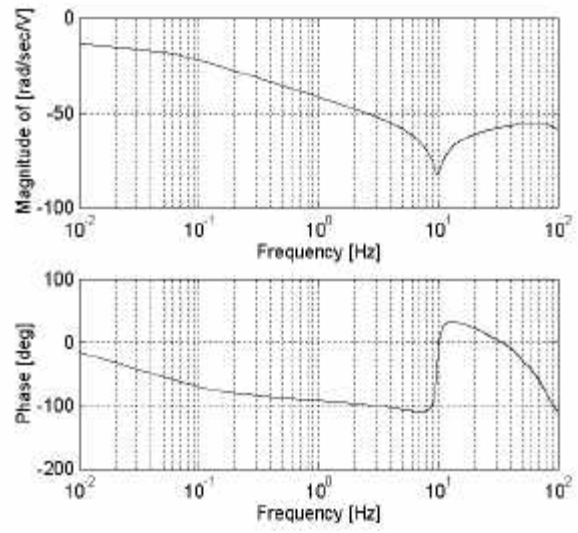

Fig. 4 - Azimuth axis: open loop transfer function bode diagram

3. REQUIREMENTS FOR AXES CONTROL

Both VST azimuth an altitude axes are controlled in a double (position and speed) feedback control loop. The speed and position controllers have to be tuned to guarantee the two most important requirements: an extremely low tracking error and a good disturbance rejection. The absolute RMS tracking error must be as low as possible in order to guarantee the image quality during the observations. Furthermore, the stability robustness of the closed loop must be guaranteed with proper gain and phase margins, to reject structural parameter changes of the controlled system and/or environment modifications. Particular attention must be paid in the synthesis of the controllers, in order to improve the guide and to assure a proper rejection against the disturbances. The main external disturbance to consider in this analysis is the wind shake. The wind mainly affects the altitude performance, because the altitude axis is subjected to a greater wind torque. The azimuth rotation is much more protected by the co-rotating enclosure. Actually most of the wind disturbance effect comes from the open slit of the enclosure in the observation direction, which affects mainly the altitude axis, and usually the influence on azimuth of the wind disturbance is neglected. The site chosen for VST, Cerro Paranal in the Atacama desert, is sometimes windy. Therefore a wind effect analysis has been carried out in the following taking into account the Chilean site weather statistics.

4. TRACKING ERROR VS IMAGE ERROR

The azimuth axis in an Alt-Az telescope can assume very high speeds when altitude axis is close to zenith, especially when crossing the meridian, where the speed reaches its maximum. On the contrary when altitude angle is low azimuth moves very slow (Mancini and Schipani, 2000). Therefore the position control can be difficult for azimuth, since the dynamic speed range is wide. The same thing does not apply to altitude axis, whose speed range is upper bounded to a low value depending on the latitude of the site: for VST the maximum speed is about 13 arcsec/sec. Usually when the speed is higher the axis error is higher too, and so it is highly probable that azimuth error is generally greater than the altitude one. But fortunately, due to geometric considerations, the influence of azimuth error on the real image error in the sky is lessened by a cos(alt) factor which becomes dominant when altitude angle approaches 90°, and so an higher error for azimuth becomes acceptable just where it arises because of the higher tracking speed.

5. CONTROLLERS

In this analysis the speed loop controller is a simple PI. The complexity of the real telescope controller could be increased by adding a series of Notch 2nd order filters in order to attenuate eventual resonant spectral components. The position controller chosen for this simulation is a standard PI controller, which ideally guarantees zero error to a ramp input (similar to the usual real observation conditions) after the transient phase. The real controller parameters will not be constant; pointing and tracking phases need different values for the proportional and integral constants. The problem can be circumvented or with a rough switch between different controller structure for small, medium and large errors, or providing the PI controller with anti-windup capability, or better with a variable structure controller (Scali, *et al.*, 1993) in which the parameters $K_p(e)$, $K_i(e)$ depend on the instantaneous position error value. This last solution has been proven to be very effective with other telescopes with similar dynamics (Mancini, *et al.*, 1997; Mancini, *et al.*, 1998). A detailed analysis of the dependence of the position controller on the tracking error is beyond the scope of the present study, which is limited to the "small" error case, i.e. to the tracking phase control. After the tuning of the position control parameters for both altitude and azimuth a -3db bandwidth of about 3 Hz has been obtained.

6. WIND DISTURBANCE EFFECT ANALYSIS

Since a telescope works in open air, partially protected by a co-rotating enclosure, the main external disturbance for a telescope is certainly the wind. Therefore the performance of a telescope position control servo system depends on its ability to minimize changes in position due to the wind. In the following an analysis of the effect of the wind

disturbance on the VST axes behavior is discussed. The altitude axis is certainly the most influenced by the wind disturbance and so most of the analysis will be focused on it.

6.1 Spectral analysis

An approach to evaluate the effect of the wind on the telescope performance is based on the description of the power spectral density of the wind by the Von Karman spectrum (Ravensbergen, 1994):

$$S_v(f) = 4(Iv)^2 \frac{L}{v} \frac{1}{\left(1+70.78\left(f\frac{L}{v}\right)^2\right)^{\frac{5}{6}}} \quad (2)$$

where v is the mean wind speed, I is the turbulence intensity, f the frequency, L the outer scale of turbulence. Three simulations have been carried out with the data shown in table 2 (where α is a wind speed reduction factor):

Table 2 – Simulation data

α	I	L [m]
1	0.15	79
0.98	0.15	3.2
0.63	0.12	3.2

These data refer to three different conditions: α=1, i.e. no wind speed reduction, shows the extreme situation of the telescope completely in open air; α=0.98 refers to the not favorable situation of the telescope observing in the direction of the wind, a scenario usually avoided whenever possible; α=0.63 refers to a more realistic situation of the telescope properly protected by the enclosure and some wind screens. The wind speed used in the simulation has been v=18 m/s; over this value no observation is usually performed in the ESO Cerro Paranal observatory. The Von Karman spectrum must be multiplied by the square of the aerodynamic correction factor χ(f):

$$c(f) = \frac{1}{1+\left(2f\frac{\sqrt{A}}{v}\right)^{\frac{4}{3}}} \quad (3)$$

where A is the exposed to the wind area. The top ring with the spiders represents the largest aerodynamic drag contribution to the torque.

$$S_w(f) = S_v(f)c^2(f) \quad (4)$$

The effect of the fluid dynamic attenuation factor is to reduce the disturbance (Fig. 6). The PSD of the torque (Fig. 7) is given by:

$$S_t(f) = 4\left(\frac{t}{v}\right)^2 S_w(f) \quad (5)$$

where τ is the wind disturbance torque. The PSD of the altitude axis rotation due to the disturbance torque (Fig. 8) can be obtained by multiplying this spectrum with the square of the disturbance transfer function D(f):

$$D(f) = \frac{q(f)}{t(f)} \quad (6)$$

$$S_J(f) = |D(f)|^2 S_t(f) \quad (7)$$

The amplitude of the disturbance as calculated with this approach depends on data mutuated from VLT wind tunnel tests and related experience. The RMS displacement error due to the torque disturbance induced by the wind is represented as a function of the bandwidth of the control loop in Fig. 9. Most of the disturbance effect is concentrated below 1Hz. Higher is the bandwidth, better is the disturbance rejection; in practice the bandwidth is limited by the dynamic of the telescope, mainly by the locked rotor frequency (Ravensbergen, 1994). The bandwidth estimated for VST is about 3Hz, sufficient to contrast effectively the wind disturbance. A better error estimation is obtained from the time domain analysis reported in the following.

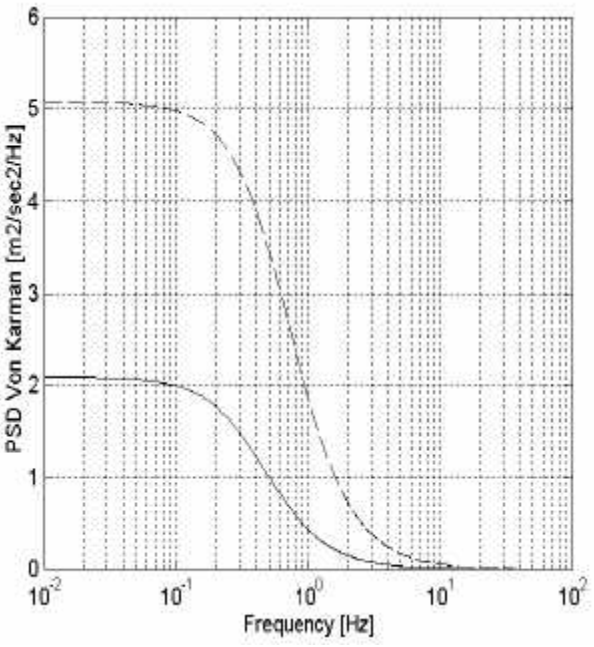

Fig. 5 - PSD of the wind speed $S_v(f)$ (α=0.98 dashed line, α=0.63 continuous line)

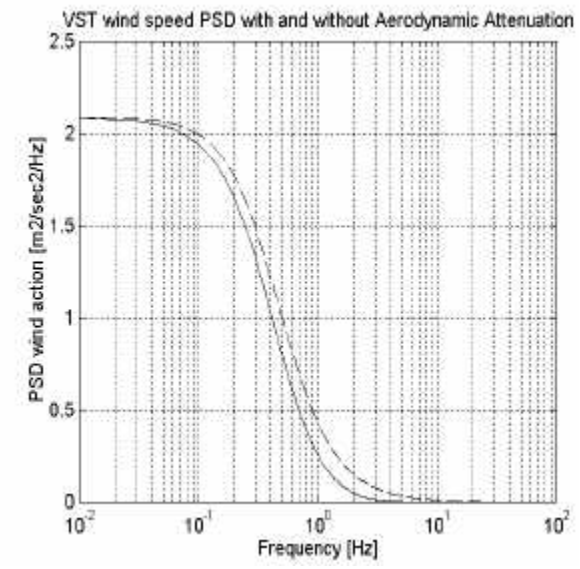

Fig. 6 - PSD of the wind speed with (continuous line) and without (dashed line) aerodynamic attenuation (α=0.63)

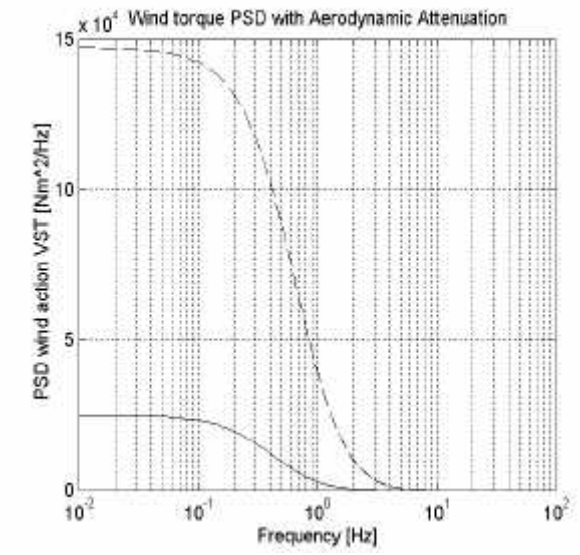

Fig. 7 - PSD of the wind torque $S_t(f)$ (α=0.98 dashed line, α=0.63 continuous line)

6.2 Time domain analysis

The wind disturbance effect has been studied in the time domain simulating a tracking at a speed of 10 arcsec/sec (almost the maximum velocity for altitude), generating torque disturbance time series as a sum of sine waves with amplitudes determined from the power spectral density and with random phases (Andersen, 1994):

$$t(t) = \sum_{1}^{N} \sqrt{2 S_t(f_k) \Delta f} \cos(2\pi f_k t + f_k)$$

where Δf = 0.01 Hz is the frequency resolution, N = 10000 the number of frequency samples, ϕ_k random phase angles. Two case studies have been considered (α=0.63, α=0.98), skipping the not realistic "open air" condition (α=1) used before only for comparison. So two sets of simulations have been carried out at increasing wind speeds. It should be considered that since observing in the direction of the wind is not a preferred scenario the α=0.63 case can be considered the more realistic observation condition, having properly set the wind screens and the whole enclosure.

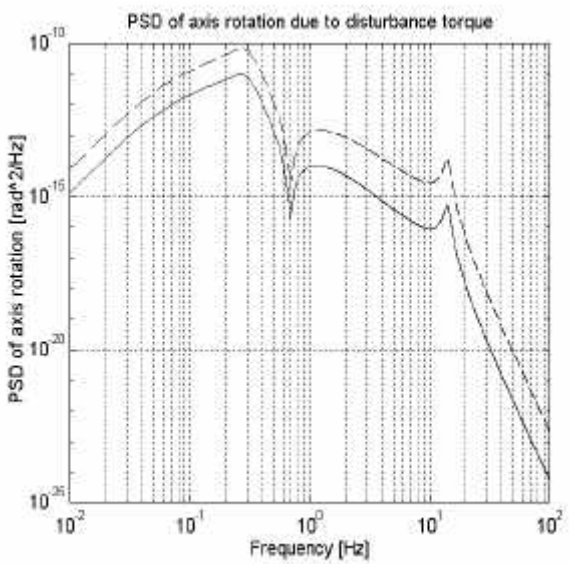

Fig. 8 - PSD of axis rotation due to the wind disturbance torque $S_q(f)$ (α=0.98 dashed line, α=0.63 continuous line)

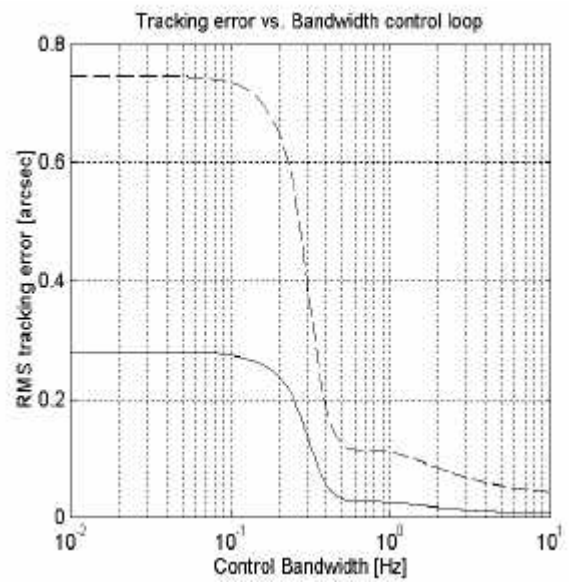

Fig. 9 - Tracking error vs bandwidth of the control loop (α=0.98 dashed line, α=0.63 continuous line)

One of the simulation time series result is shown in Fig. 10. The interpolation of the data results is reported in Fig. 11. Table 3 reports also the percentage of time in which the wind in Paranal is above the selected wind speed (Sarazin, 1999).

Table 3 - RMS tracking errors due to wind disturbance

V [m/s]	Time % With Wind Speed > V	RMS Tracking Error (α=0.98) [arcsec]	RMS Tracking Error (α=0.63) [arcsec]
3	77	0.02	0.005
6	50	0.10	0.03
9	24	0.30	0.09
12	11	0.54	0.16
15	5	0.80	0.26
18	2	1.10	0.38

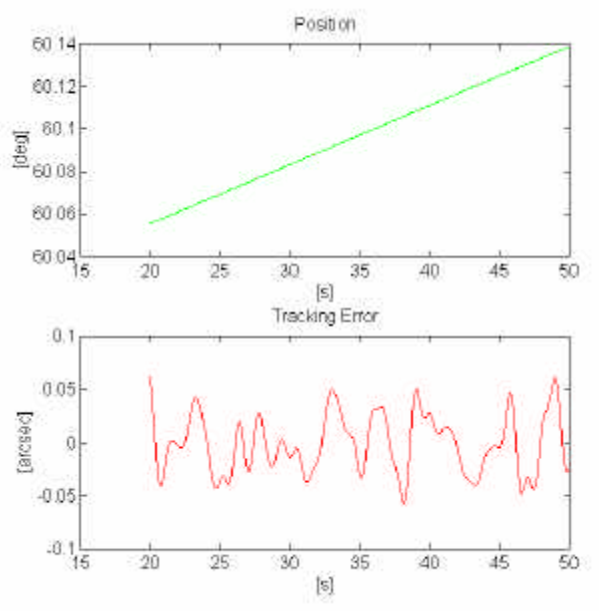

Fig. 10 - Altitude tracking error (wind speed=6m/s, α=0.63)

7. CONCLUSIONS

For a telescope of the same class of the VST usually the maximum admitted tracking RMS error is about 0.15 arcsec, a value which does not affect the image quality even in good seeing conditions. According to this simulation results the disturbance effect would increase with wind speed as foreseen; in the α=0.63 case up to 12 m/s the effect could be considered not really performance limiting even in good seeing conditions, while at higher wind speeds in very good seeing conditions a negative effect could be noticed. The problem anyway should be limited to a low percentage of telescope usage time; the wind speed is above 12 m/s in about 11% of the time, above 15 m/s only in the 5% of the time. During the most windy nights, it is possible to re-schedule the less performance demanding observation programs, i.e. engineering tests on the telescope and its instrumentation. In very windy nights further improvements in the image quality could be obtained implementing fast mirror position correction techniques, external to the axes control system.

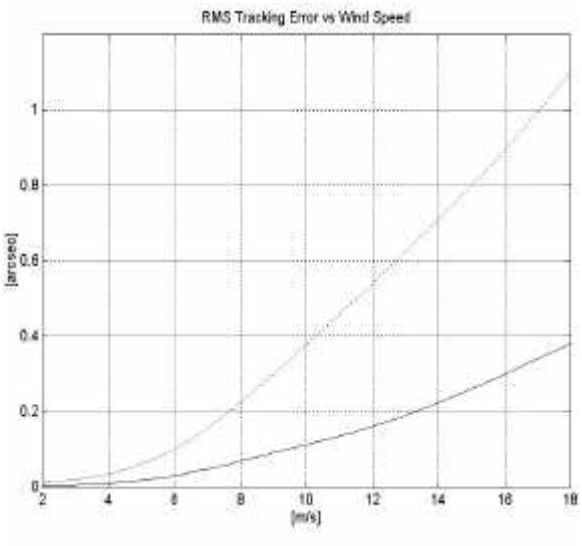

Fig. 11 - RMS tracking error vs wind speed (α=0.98 upper line, α=0.63 lower line)

REFERENCES

Andersen, T. The Servo System of the EISCAT Svalbard Antenna. Proceedings of SPIE, **2479**, 301

Mancini, D., Brescia, M., Cascone, E., and Schipani, P (1997). A variable structure control law for telescopes pointing and tracking. In: *Acquisition, Tracking, and Pointing XI* (M. K. Masten, L. A. Stockum, Eds.). Proceedings of SPIE, **3086**, 72

Mancini, D., Cascone, E., and Schipani, P. (1998). Telescope control system stability study using a variable structure controller. In *Telescope Control System III* (H. Lewis, Ed.). Proceedings of SPIE, **3351**, 341

Mancini, D., Schipani, P. (2000). Tracking performance of the TNG Telescope. In *Advanced Telescope and Instrumentation Control Software* (Lewis, H., Ed.). Sproceedings of SPIE, **4009**, 355

Ravensbergen, M. (1994). Main axes servo systems of the VLT, Proceedings of SPIE, **2199**, 997

Sarazin, M. (1999). Wind at Paranal: Nighttime Velocity Histogram (1985-1999). http://www.eso.org

Scali, C., Nardi, G., Landi, A., and Balestrino, A. (1993). Performance of variable structure PI controllers in presence of uncertainty and saturation nonlinearities. XII IFAC World Congress, Vol. **8**, 527, Sidney